# Fubini instantons in curved space

Bum-Hoon Lee[a,b*], Wonwoo Lee[b†], Changheon Oh[c‡], Daeho Ro[a§]
and Dong-han Yeom[b,d¶]

[a]*Department of Physics and BK21 Division, Sogang University, Seoul 121-742, Korea*
[b]*Center for Quantum Spacetime, Sogang University, Seoul 121-742, Korea*
[c]*Meerecompany, Gyeonggi-do 445-938, Korea*
[d]*Yukawa Institute for Theoretical Physics, Kyoto University, Kyoto 606-8502, Japan*

September 17, 2018

## Abstract

We study Fubini instantons of a self-gravitating scalar field. The Fubini instanton describes the decay of a vacuum state under tunneling instead of rolling in the presence of a tachyonic potential. The tunneling occurs from the maximum of the potential, which is a vacuum state, to any arbitrary state, belonging to the tunneling without any barrier. We consider two different types of the tachyonic potential. One has only a quartic term. The other has both the quartic and quadratic terms. We show that, there exist several kinds of new O(4)-symmetric Fubini instanton solution, which are possible only if gravity is taken into account. One type of them has the structure with $Z_2$ symmetry. This type of the solution is possible only in the de Sitter background. We discuss on the interpretation of the solutions with $Z_2$ symmetry.

[*]`bhl@sogang.ac.kr`

[†]`warrior@sogang.ac.kr`

[‡]`choh0423@gmail.com`

[§]`dhro@sogang.ac.kr`

[¶]`innocent.yeom@gmail.com`

# 1 Introduction

The very first picture of an inflationary multiverse scenario was proposed in Ref. [1], in which it would seem that the author wanted to suggest a universe without the cosmological singularity problem using an interesting feature of self-reproducting or regenerating exponential expansion of the universe. A major development in this scenario was triggered by the discovery of the eternal inflationary scenario [2–5] and a paradigm for string theory landscape [6,7]. The eternal inflation is related to the expanding false vacuum solution with a positive cosmological constant, which in turn means that the inflation is eternal into the future. If the theory has multiple minima then the false vacuum state decays into the true vacuum state, i.e. the phase transition proceeded *via* the nucleation of a vacuum bubble. In this scenario the universe is situated within some bubble called a pocket universe [4] having a certain value of the cosmological constant and the whole universes are referred to as multiverse. The description of self-reproduction including tunneling process and random walk was combined into a scenario called recycling universe [8]. These scenarios seem to provide an escape from the question of the initial conditions of the universe, i.e. it seems to be eternal into the past. Unfortunately, inflationary spacetimes cannot be made complete in the past direction [9], even though the universe is eternal into the future. There are still interesting arguments on the beginning of the universe [10]. The string theory landscape is a setting that involves a huge number of different metastable and stable vacua [11,12], originated from different choices of Calabi-Yau manifolds and generalized magnetic fluxes. The huge number of different vacua can be approximated by the potential of a scalar field. The important thing is the fact that, once the de Sitter vacuum can exist, the inflationary expansion is eternal into the future and has the possibility of self-reproduction.

On the other hand, there are theories of gauged $d = 4$, $N = 8$ supergravity having de Sitter(dS) solution, in which all SUSYs are spontaneously broken. It is well known that the dS solution corresponds to a M/sting theory solution with a non-compact 7- or 6-dimensional internal space, in which a small value of the cosmological constant stems from the 4-form flux. The simplest representative of these kind of theories has a tachyonic potential with the dS maxima [13–15]. The potential in the vicinity of the maximum reduces to a form having a quadratic term, that is not metastable but unstable. However, according to some authors, the time for collapse giving rise to the tachyonic potential can be much greater than the age of the universe for anthropic reasoning. If the curvature radius of the potential in the vicinity of the maximum is greater than that used in the above theory, then that will be all together different story. The supergravity analogue of the tachyonic potential could be constructed also by using an exact supergravity solution representing the $D_p$-$\bar{D}_p$ system [16].

From the above scenarios, the study of the possibility of the tunneling process for the potential with stable and metastable vacua, or even tachyonic behavior has acquired renewed interest. In the present paper, we will study the tunneling process under a simple tachyonic potential governed by a quartic term both without the quadratic term and with the term as a toy model. To obtain the general solution including the effect of the backreaction, we solve the coupled equations for the gravity and the scalar field simultaneously. Although the model has

a tachyonic potential, it might still be an useful example to show how the tunneling process occurs in various shapes of the potential provided by the above scenarios.

A quantum particle can tunnel through a finite potential barrier *via* the so-called barrier penetration. This process can be described by the Euclidean solution obeying appropriate boundary conditions. There exist two kinds of Euclidean solutions describing quantum tunneling phenomena. One corresponds to an instanton solution representing a stable pseudoparticle configuration characterized by the existence of a nontrivial topological charge. It does not change even if we continuously deform the field, as long as the boundary conditions remain the same. The instanton solution corresponds to the minimum of the Euclidean action to pass from the initial to final state [17]. The solution, in case of a double well potential, describes a general shift in the ground state energy of the classical vacuum due to the presence of an additional potential well, then lifting the so-called classical degeneracy. The other is a bounce solution representing an unstable nontopological configuration that corresponds to a saddle point rather than a minimum of the Euclidean action. The second derivative of the Euclidean action around the bounce has one negative eigenvalue which leads to the imaginary part of the energy. The existence of the negative eigenvalue implies that the vacuum state is unstable, i.e. the state decays into other states [18].

The Euclidean solutions can also mediate phase transitions. The phase transition describes the sudden change of a physical system from one state to another. The transition are of two different types transition accompanied by temperature or zero temperature. The competition between the entropy and the energy terms in the thermodynamic potential cause thermal phase transitions in which dynamics is irrelevant. In the modern classification scheme, thermal phase transitions are divided into two broad categories either with a discontinuous jump in the first-order derivatives of the free energy or without it. A first-order phase transition is characterized by the discontinuity in the first derivative of the free energy and is associated with the existence of latent heat, whereas a $n$th-order phase transition is characterized by the continuity in the first derivative while there is a discontinuity in the $n$th-order derivative. A quantum phase transition describes a transition between different phases by quantum fluctuation, which occurs at zero temperature, unlike the case of a thermal phase transition which is governed by a thermal fluctuation [19].

To simplify things, we consider an asymmetric double well potential to distinguish two different phase transitions at zero temperature. If the initial state is the metastable vacuum state and the tunneling occurs from that state to the other vacuum state, then the transition corresponds to a tunneling process [20–25]. On the other hand, if the initial state is the local maxima of the potential and the field is rolling down to one vacuum state continuously rather than any discontinuous jump, then the transition corresponds to the rolling. However, one more channel exists as tunneling and that corresponds to the one without a barrier. In this kind of transition, the initial state on the top of a potential can tunnel to the other state rather than rolling down the potential [26–28, 30]. There are two different kind of transitions in this case. One is the tunneling without a barrier representing the tunneling from the local maximum of the potential to the vacuum state [28–31]. Recently, an analytic study on this

type of solution was performed in [31]. The other is a tunneling without a barrier representing the tunneling from the maximum of the potential to any arbitrary state. This case corresponds to the Fubini instanton [26, 27], where the tachyonic potential is employed. Can we describe the rolling corresponding to the transition between the initial metastable vacuum state and the other final vacuum state? This may look similar to a superfluid motion by the liquid helium. Although to establish the phase transition corresponding to the superfluid motion is itself a very challenging problem, we concentrate on the Fubini instantons in this work.

The Fubini instanton [26, 27] describes the decay of a vacuum state by the quantum phase transition instead of rolling down the tachyonic potential consisted of a quartic term only. On the other hand, one can consider a tachyonic potential consisted of a quadratic term only, the point $\Phi = 0$ is unstable. A small perturbation will cause it to roll down the hill of the potential. Originally, it was Fubini who introduced a fundamental scale of hadron phenomena by means of the dilatation noninvariant vacuum state in the framework of a scale invariant Lagrangian field theory [26]. However, the solution is a one-parameter family of instanton solutions representing a tunneling without a barrier as an interpolating solution from the maximum of the potential to any arbitrary state. The instanton solution was studied in a conformally invariant model, i.e. a fixed background was used and the effect of the backreaction by instantons was neglected [32–34]. This is a good approximation, when the variation of the potential during the transition is much smaller than the maximum of the potential. The instanton has gained much interest now-a-days in the context of anti-de Sitter(AdS)/conformal field theory correspondence [35, 36].

The paper is organized as follows: In Sec. 2, we review the Fubini instanton in the absence of gravity. We present numerical solutions including the Euclidean energy density as an example and analyze the structure of the solution in the theory with a potential having only the quartic self-interaction term. We stress the fact that there is no such solutions with the potential containing both the quartic and the quadratic terms. In Sec. 3, we show that the instanton solutions exist in the curved space. We perform a numerical study to solve the coupled equations for the gravity and the scalar field simultaneously. We show that there exist numerical solutions without oscillation in the initial AdS space in the potential with only the quartic term. We also show that there exist numerical solutions in the potential both with the quartic and the quadratic terms irrespective of the value of the cosmological constant, which is possible only when the gravity is switched on. In order to estimate the decay rate of the background state, we compute the action difference between that of the solution and the background obtained by numerical means. We present an oscillating numerical solutions in the potential with only the quartic term with various values of the cosmological constant. One type of these solutions has the structure with $Z_2$ symmetry. We will discuss on the interpretation of the solutions with $Z_2$ symmetry in the final Section. We analyze the behavior of the solutions using the phase diagram method. In Sec. 4, to observe the dynamics of the solutions, we briefly sketch the causal structures of the solutions in the Lorentzian spacetime. Finally in Sec. 5, we summarize and discuss our results.

4

# 2 Fubini instanton in the absence of gravity

One can consider the following action in the absence of gravity

$$S = \int_{\mathcal{M}} \sqrt{-g} d^4 x \left[ -\frac{1}{2} \nabla^\alpha \Phi \nabla_\alpha \Phi - U(\Phi) \right], \tag{1}$$

where $g = \det \eta_{\mu\nu}$, $\eta_{\mu\nu} = diag(-1, 1, 1, 1)$ is the Minkowski metric, and the tachyonic potential has a quartic self-interaction term and also a quadratic term as follows:

$$U(\Phi) = -\frac{\lambda}{4} \Phi^4 + \frac{m^2}{2} \Phi^2 + U_o, \tag{2}$$

where $m^2 > 0$ and $\lambda > 0$. The plots of potentials (a) without the quadratic term and (b) with the quadratic term are shown in Fig. 1. The potential has a metastable vacuum state at $\Phi = 0$ and no other stationary state in Fig. 1(a), while Fig. 1(b) illustrates that the potential has a local minimum at $\Phi = 0$ and two maxima [27, 37, 38]. In both the cases, the potential is not bounded from below.

Before going to the tunneling problem in four dimensions, we briefly describe the problem in one dimension. One can consider the simplest quantum tunneling problem in one dimension. Quantum field theory in one dimension is nothing but ordinary quantum mechanics. In case of $m^2 = 0$, the amplitude for transmission obeys the WKB formula in the semiclassical approximation, in which $\Phi_\pm = \pm(\frac{4U_o}{\lambda})^{1/4}$ are the classical turning points. On the other hand, the double-hump potential with $m^2 > 0$ and $U_o = 0$ can be considered as an inverted double-well potential for a bounce solution representing the tunneling from $\Phi = 0$ to $\Phi_\pm = \pm m\sqrt{2/\lambda}$. The solution is given by $\Phi_s(\tau) = \pm m\sqrt{2/\lambda}\text{sech}[m(\tau - \tau_o)]$, where $\tau_o$ is an integration constant. The bounce solutions can be easily understood in the Euclidean space. The particle can only reach the point $\Phi = 0$ at $\tau = \pm\infty$ and it bounces off $\Phi_\pm = \pm m\sqrt{2/\lambda}$ at $\tau = 0$ with a vanishing velocity [39].

We now turn to the tunneling problem in four dimensions. It is an well-known fact that the massless theory has an instanton [26]. Actually, the instanton corresponds to the bounce solution representing the decay of the background vacuum state. The equation of motion with $O(4)$ symmetry, obtained by varying the Euclidean action, is then;

$$\frac{d^2\Phi}{d\eta^2} + \frac{3}{\eta}\frac{d\Phi}{d\eta} = -\frac{d(-U)}{d\Phi}, \tag{3}$$

where $\eta(= \sqrt{\tau^2 + x^2})$ plays the role of the evolution parameter in Euclidean space and the second term in the left-hand side plays the role of a damping term. The boundary conditions are

$$\frac{d\Phi}{d\eta}\bigg|_{\eta=0} = 0 \quad \text{and} \quad \Phi|_{\eta=\infty} = 0. \tag{4}$$

The particle in the classical mechanics problem starts at $\Phi = \Phi_o$ with zero velocity in the inverted potential, and stops at $\Phi|_{\eta=\infty} = 0$ without any oscillation.
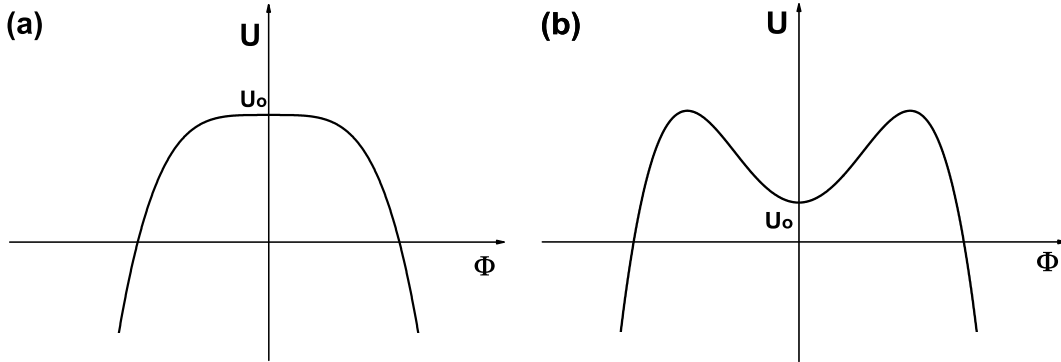
Figure 1: Potentials for the case of (a) Fubini instantons and (b) generalized Fubini instantons.

For the potential with $m^2 = 0$, the analytic solution of the Fubini instanton has the form

$$\Phi(\eta) = \sqrt{\frac{8}{\lambda}} \frac{b}{\eta^2 + b^2} \, , \tag{5}$$

where $\eta$ is the radial length in the Euclidean space, $b$ is any arbitrary length scale which characterizes the size of the instanton and is related to the initial value $\Phi_o$. In addition, the value of the scalar field of the center of the solution depends on $b$ as $\Phi(0) = \sqrt{\frac{8}{\lambda}\frac{1}{b}}$. This solution was used in the related perturbation theory [40].

The characteristic behavior of the analytic solution is ploted in Fig. 2 in terms of the value of the parameter $b$. We take $\lambda = 1$ for all the cases. The solid line denotes the solution with $b = 1$, the dashed line with $b = 3$, and the dotted line with $b = 5$. The corresponding Euclidean action is given by

$$S_{\mathrm{E}} = \frac{32\pi^2 b^2}{\lambda} \int_0^\infty \frac{\eta^5(1 - \frac{b^2}{\eta^2})}{(\eta^2 + b^2)^4} d\eta = \frac{8\pi^2}{3\lambda} \, , \tag{6}$$

where the action does not depend on the parameter $b$ due to the consequence of the conformal invariance of the potential and we take that value to be $U_o = 0$. The action has the same value irrespective of the starting point $\Phi_o$. In other words, the tunneling from the maximum of the potential to any arbitrary state always happens with same probability.

The numerical solutions for $\Phi$ and $\Phi'$ and the Euclidean energy including the density variation with $\eta$ are as shown in Fig. 3. Figure 3(a) illustrates the numerical solution for $\Phi$, in which the initial value set as $\Phi_o = -1$ and the solution asymptotically approaches the value $\Phi = 0$. Figure 3(b) illustrates $\Phi'$ with respect to $\eta$. There is a peak of $\Phi'$ near $\eta = 2.31$. Figure 3(c) depicts the volume energy density, when the density has got the form $\xi = [\frac{1}{2}\Phi'^2 + U]$. The lower
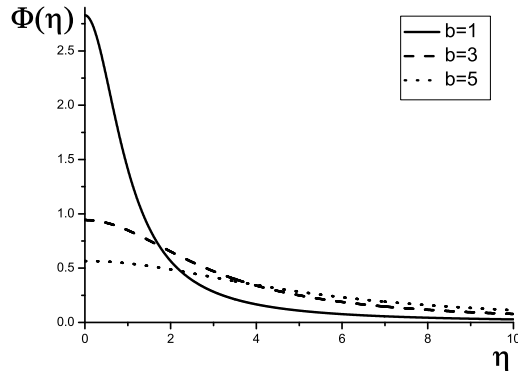
6

Figure 2: The analytic solution of the Fubini instanton in absence of gravity.

right box in the same figure shows the magnification of the small region clearly representing the existence of a smooth hill. The smooth peak of the volume energy density exists at $\eta = 5.17$. There is a disagreement between the location of the peak for the energy density and that for $\Phi'$. It clearly reveals the fact that the position with the maximum value for $\Phi'$ is still not the same as the maximum of the energy density due to non-trivial contribution coming from the potential, $U = -\frac{\lambda}{4}\Phi^4$. Figure 3(d) shows the Euclidean energy $E_\xi$ for each slice of constant $\eta$. The Euclidean energy signifies the value of energy after the full integration of variables except for $\eta$ in the present work, $E_\xi = 2\pi^2\eta^3\xi$. There are one minimum and one maximum point for $E_\xi$. The location of the minimum of $E_\xi$ is around $\eta = 2.31$, whereas that of the maximum is near $\eta = 6.93$. Ironically, the location of the minimum of $E_\xi$ coincides with that of the maximum of $\Phi'$. These solutions can be considered as a ball consisting of only a thick wall except for one point at the center of the solution with a lower arbitrary state than the outer vacuum state unlike a vacuum bubble that consists of an inside part with a lower vacuum state and a wall.

For a theory with $m^2 > 0$, the conformal invariance is broken and any solution with a finite action is forbidden by scaling argument. In other worlds, the particle can not have enough energy to reach the hill overcome the barrier near $\Phi = 0$ since the damping term has got a large value due to a large value of $\Phi'$ near the initial point [41].

## 3 Fubini instantons of a self-gravitating scalar field

Let us consider the following action:

$$S = \int_{\mathcal{M}} \sqrt{-g}d^4x \left[\frac{R}{2\kappa} - \frac{1}{2}\nabla^\alpha\Phi\nabla_\alpha\Phi - U(\Phi)\right] + \oint_{\partial\mathcal{M}} \sqrt{-h}d^3x\frac{K - K_o}{\kappa}, \tag{7}$$

7

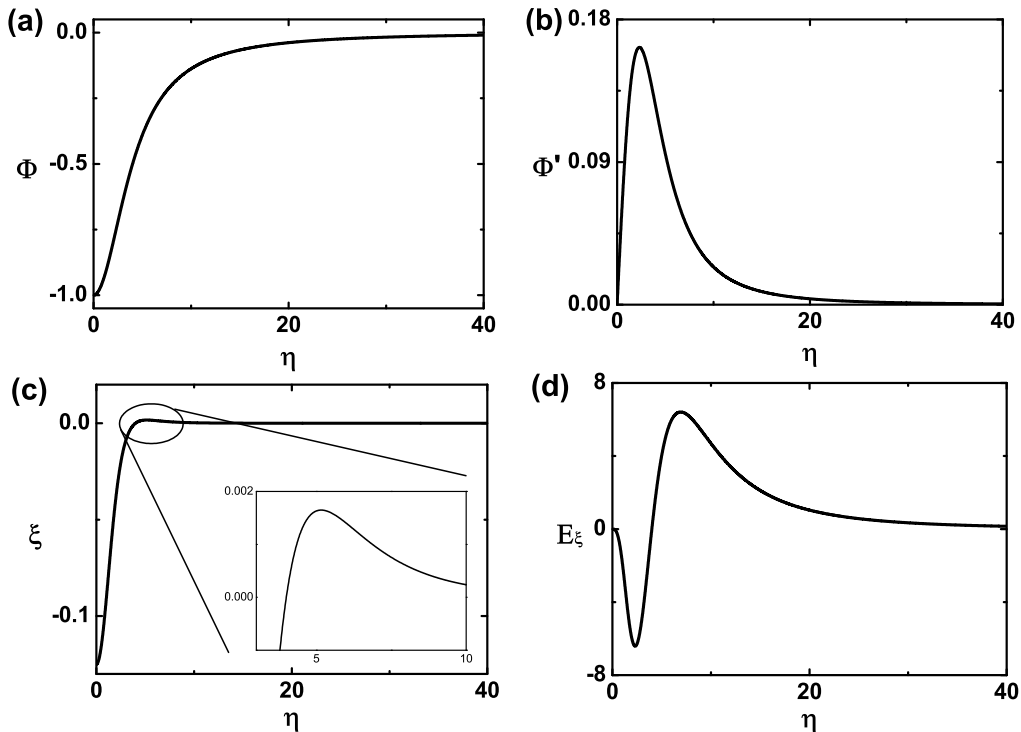Figure 3: (a) The numerical solution for $\Phi$ in the case of $m^2 = 0$, (b) the variation of $\Phi'$ with respect to $\eta$, (c) the energy density $\xi$ and (d) the Euclidean energy $E_\xi$ evaluated at constant $\eta$.

where $g = \det g_{\mu\nu}$, $\kappa \equiv 8\pi G$, $R$ denotes the scalar curvature of the spacetime $\mathcal{M}$, $h$ is the induced boundary metric, $K$ and $K_o$ are the traces of the extrinsic curvatures of $\partial\mathcal{M}$ for the metric $g_{\mu\nu}$ and $\eta_{\mu\nu}$, respectively. The second term on the right-hand side is the boundary term [42]. It is necessary to have a well-posed variational problem including the Einstein-Hilbert term. Here we adopt the notations and sign conventions of Misner, Thorne and Wheeler [43].

We study the creation process of Fubini instantons in curved spacetime. In the first place, we consider the massless case, and then we will also consider generalized Fubini instantons, the so-called massive case (see the form of the potential in Eq. (2)). The cosmological constant is given by $\Lambda = \kappa U_0$, such that background space will be dS, flat or AdS depending on the signs of $U_0$.

In order to solve the coupled equations, we assume an $O(4)$ symmetry for the geometry and the scalar field similar to Ref. [22]

$$ds^2 = d\eta^2 + \rho^2(\eta) \left[ d\chi^2 + \sin^2\chi \left( d\theta^2 + \sin^2\theta d\phi^2 \right) \right] . \tag{8}$$

And then, $\Phi$ and $\rho$ depends only on $\eta$, and the Euclidean equation can be written respectively as follows:

$$\Phi'' + \frac{3\rho'}{\rho}\Phi' = \frac{dU}{d\Phi} \quad \text{and} \quad \rho'' = -\frac{\kappa}{3}\rho(\Phi'^2 + U) \,, \tag{9}$$

and the Hamiltonian constraint is then given by

$$\rho'^2 - 1 - \frac{\kappa\rho^2}{3}\left(\frac{1}{2}\Phi'^2 - U\right) = 0 \,. \tag{10}$$

In order to yield a meaningful solution, the constraint requires a delicate balance among all the different terms. Otherwise the solution can yield qualitatively incorrect behavior [44].

To solve the Eqs. (9), we have to impose suitable boundary conditions. When the gravity is switched off, boundary conditions for the Fubini instanton are $\frac{d\Phi}{d\eta}\big|_{\eta=0} = 0$ and $\Phi|_{\eta=\infty} = 0$ as in Ref. [26]. While gravity is taken into account, we can write boundary conditions as follows:

$$\rho|_{\eta=0} = 0, \quad \frac{d\rho}{d\eta}\bigg|_{\eta=0} = 1, \quad \frac{d\Phi}{d\eta}\bigg|_{\eta=0} = 0, \quad \text{and} \quad \Phi|_{\eta=\eta_{max}} = 0 \,, \tag{11}$$

where $\eta_{max}$ is the maximum value of $\eta$. For the flat and AdS background $\eta_{max} = \infty$, while $\eta_{max}$ is finite for the dS background. The first condition is to obtain a geodesically complete spacetime. The second condition is nothing but Eq. (10). The third condition is the regularity condition as can be seen from the first equation in Eq. (9). One should find the undetermined initial value of $\Phi$, i.e. $\Phi|_{\eta=0} = \Phi_o$, using the undershoot-overshoot procedure [21,30], to satisfy the fourth condition $\Phi|_{\eta=\eta_{max}} = 0$. We employ these conditions for Fubini instantons in Sec. III A, B.

If the background space is dS, we can impose conditions specified at $\eta = 0$ and $\eta = \eta_{max}$. For this purpose, we choose the values of the field $\rho$ and derivatives of the field $\Phi$ as follows:

$$\rho|_{\eta=0} = 0, \quad \rho|_{\eta=\eta_{max}} = 0, \quad \frac{d\Phi}{d\eta}\bigg|_{\eta=0} = 0, \quad \text{and} \quad \frac{d\Phi}{d\eta}\bigg|_{\eta=\eta_{max}} = 0. \tag{12}$$

The first two conditions are for the background space. The last two conditions are for the scalar field. In general, the solutions satisfying Eq. (12) do not guaranty $\Phi_{\eta=\eta_{max}}$ to be zero. For the solution having $\Phi_{\eta=\eta_{max}} = 0$, the conditions Eq. (12) are equivalent to the conditions Eq. (11). If $\Phi_{\eta=\eta_{max}} = \pm\Phi_o$, they represent completely new type of solutions with $Z_2$ symmetry. We will discuss this case more in detail in Sec. III C.

In order to solve the Euclidean field Eqs. (9) and (10) numerically, we rewrite the equations in terms of dimensionless variables as in Ref. [30]. In the present work, we employ the shooting method using the adaptive step size Runge-Kutta as the integrator similar to the treatment in Ref. [45]. For this procedure we choose the initial values of $\tilde{\Phi}(\tilde{\eta}_{\text{initial}})$, $\tilde{\Phi}'(\tilde{\eta}_{\text{initial}})$, $\tilde{\rho}(\tilde{\eta}_{\text{initial}})$, and

9

$\tilde{\rho}'(\tilde{\eta}_{\text{initial}})$ at $\tilde{\eta} = \tilde{\eta}_{\text{initial}}$ as follows:

$$
\begin{aligned}
\tilde{\Phi}(\tilde{\eta}_{\text{initial}}) &\sim \tilde{\Phi}_o - \frac{\epsilon^2}{8}\tilde{\Phi}_o(\tilde{\Phi}_o^2 - 1) + \cdots, \\
\tilde{\Phi}'(\tilde{\eta}_{\text{initial}}) &\sim -\frac{\epsilon}{4}\tilde{\Phi}_o(\tilde{\Phi}_o^2 - 1) + \cdots, \\
\tilde{\rho}(\tilde{\eta}_{\text{initial}}) &\sim \epsilon + \cdots, \\
\tilde{\rho}'(\tilde{\eta}_{\text{initial}}) &\sim 1 + \cdots,
\end{aligned}
\tag{13}
$$

where $\tilde{\eta}_{\text{initial}} = 0 + \epsilon$ for $\epsilon \ll 1$. The minus sign in front of the second formula is due to the negative value of the $\tilde{\Phi}''$ determined by the sign of $dU/d\Phi$ at $\tilde{\eta} = 0$. However, the initial value of $\tilde{\Phi}'$ is taking to be positive in the present work. Once we specify the initial value $\tilde{\Phi}_0$, the remaining conditions can be exactly determined from Eqs. (13). Furthermore we impose additional conditions implicitly. To avoid a singular solution at $\tilde{\eta} = \tilde{\eta}_{\text{max}}$ for the Euclidean field equations and to demand a $Z_2$ symmetry, the conditions $d\tilde{\Phi}/d\tilde{\eta} \to 0$ and $\tilde{\rho} \to 0$ as $\tilde{\eta} \to \tilde{\eta}_{\text{max}}$ are needed in the next section. In this work, we require that the value of $d\tilde{\Phi}/d\tilde{\eta}$ goes to a value smaller than $10^{-6}$ as $\tilde{\eta} \to \tilde{\eta}_{\text{max}}$, as the exact value of $\tilde{\eta}_{\text{max}}$ is not known [30]. The parameter $\tilde{\kappa}$ is the ratio between the gravitational constant or Planck mass and the mass scale in the theory, $\tilde{\kappa} = \frac{m^2}{\lambda}\kappa = \frac{8\pi m^2}{M_p^2 \lambda}$, and the parameter $\tilde{\kappa}\tilde{U}_o$ is related to the rescaled cosmological constant $\Lambda/m^2$.

To find the probability of the instanton solution, we only consider the Euclidean action for the bulk part in Eq. (7) to get,

$$
S_E = \int_{\mathcal{M}} \sqrt{g_{\text{E}}}d^4 x_{\text{E}} \left[ -\frac{R_{\text{E}}}{2\kappa} + \frac{1}{2}\Phi'^2 + U \right] = 2\pi^2 \int \rho^3 d\eta [-U],
\tag{14}
$$

where $R_{\text{E}} = 6[1/\rho^2 - \rho'^2/\rho^2 - \rho''/\rho]$. We used Eqs. (9) and (10) to arrive at this. The volume energy density has the form: $\xi = -U$, which has a different sign compared to the sign of the density used in Ref. [30]. The Euclidean energy signifies the energy value after the full integration of variables except for $\eta$ in the present case as $E_\xi = 2\pi^2 \rho^3 \xi$.

In the beginning, we obtain the numerical solution for $m^2 = 0$. And then we obtain the numerical solution for $m^2 > 0$. We call the space dS when the initial vacuum state has a positive cosmological constant, $U_o > 0$, flat when $U_o = 0$ and AdS when $U_o < 0$.

The rate of decay of a metastable state can be evaluated in terms of the classical configuration and represented as $Ae^{-B}$ in this approximation, in which the leading semiclassical exponent $B = S^{\text{cs}} - S^{\text{bg}}$ is the difference between the Euclidean action corresponding to the classical solution $S^{\text{cs}}$ and the background action $S^{\text{bg}}$. The prefactor $A$ is evaluated from the Gaussian integral over fluctuations around the background classical solution [46, 47].

## 3.1 Solutions without oscillation

We perform the numerical work with $m^2 = 0$ and take $\tilde{\kappa} = 0.1$. The solutions without oscillation are only possible in the initial AdS background as shown in Fig. 4. We guess that there is no
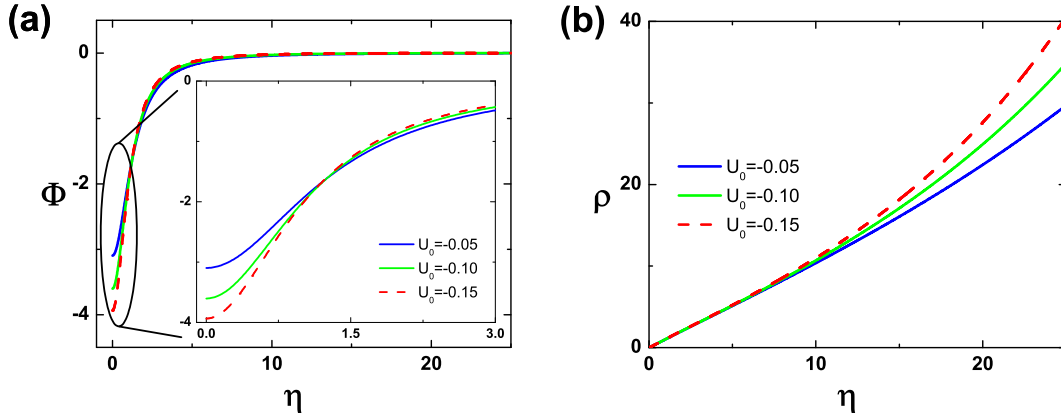
Figure 4: (color online). The numerical solutions of Fubini instantons with $m^2 = 0$ in the AdS space.

| $\tilde{U}_0$ | $\tilde{\Phi}_0$ | Color of plot | $S^{\text{cs}}$ | $S^{\text{bg}}$ | B |
|---|---|---|---|---|---|
| $-0.05$ | $-3.09706$ | Red | $1.38470 \times 10^5$ | $1.36162 \times 10^5$ | $2.30801 \times 10^3$ |
| $-0.10$ | $-3.60269$ | Green | $3.91419 \times 10^5$ | $3.82936 \times 10^5$ | $8.48298 \times 10^4$ |
| $-0.15$ | $-3.93551$ | Blue | $8.25148 \times 10^5$ | $8.03225 \times 10^5$ | $2.19226 \times 10^4$ |

Table 1: The dimensionless variables and color of plot used and the actions obtained in Fig. 4.

solution without any oscillation for the initial flat and dS background. In the given $\tilde{\kappa}$, there may exist the phase space of solutions having the region of an arbitrary $\Phi_o$. If $\tilde{\kappa}$ is increased, the oscillating behavior is appearing in the phase space of solutions [48].

Figure 4(a) illustrates the solution for $\tilde{\Phi}$, in which the right box in the same figure shows the magnification of a small region representing the initial values of $\tilde{\Phi}$ and the behavior of the curves. The curves move upwards with increasing value of $\tilde{U}_o$, then overlap near $\tilde{\eta} = 1$, and more downwards with increasing value of $\tilde{U}_o$. Figure 4(b) shows the solutions of $\tilde{\rho}$. The curves move downwards with increasing $\tilde{U}_o$. The shape of the numerical solution $\tilde{\rho}$ can be easily understood if one thinks of the shape of the solution in a fixed AdS space as $\rho = \sqrt{\frac{3}{\Lambda}} \sinh \sqrt{\frac{\Lambda}{3}} \eta$. Table 1 shows the dimensionless variables and the color of plot used, and also the actions obtained from Fig. 4. From the numerical data, one can easily see that the magnitude of $\tilde{\Phi}_o$ approaches the vacuum state $\tilde{\Phi} = 0$ as $\tilde{U}_o$ approaches a vanishing value. The vanishing of $\tilde{U}_o$ means the background geometry which serves as the initial vacuum state is flat. The action difference $\tilde{B}$
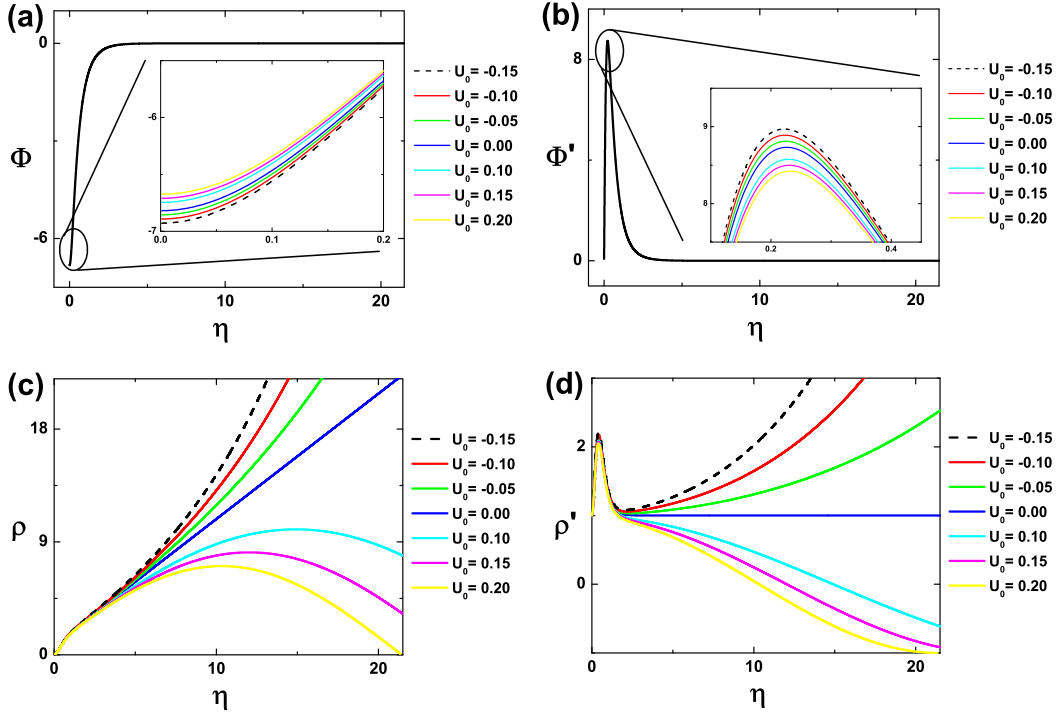
Figure 5: (color online). The numerical solution of $\Phi$, the derivative of $\Phi$ with respect to $\eta$, $\rho$, and the derivative of $\rho$ with respect to $\eta$ for the generalized Fubini instantons with $m^2 > 0$.

between the action of the solution $\tilde{S}^{\text{cs}}$ and that of the background $\tilde{S}^{\text{bg}}$ has positive values. We carry out the action integral in the range $0 \leqq \tilde{\eta} \leqq 25$ numerically as the action difference $\tilde{B}$ diverges to infinity if we perform the integration for an infinite $\tilde{\eta}$ value. This divergence is due to the fact that the size of the solution including the outside part in the evolution parameter space decrease compared to the size of the initial background similar to what happens for the case of the nucleation of a vacuum bubble. In the analytic computation, the outside part and the background are simply canceled at the same radius. In the present numerical work, it is difficult to decide the exact size of the solution. Thus we straightforwardly compute the action difference and then the difference $\tilde{B}$ has got an approximate behavior $\delta(\sinh^3 \tilde{\eta}) = 3 \sinh^2 \tilde{\eta} \cosh \tilde{\eta}$ which cause the divergence at infinity. If this minor error is cured, the action difference has a finite value.

Now we perform the numerical work with $m^2 > 0$ and take $\tilde{\kappa} = 0.3$. This type of solutions belongs to usual tunneling with a barrier. We obtained the numerical solutions with an arbitrary cosmological constant as shown in Fig. 5. The solutions are only possible for specific $\tilde{\Phi}_o$s.

The figures represent the vary fact that the solution is only possible in curved spacetime

| $\tilde{U}_0$ | $\tilde{\Phi}_0$ | Color of plot | $S^{\text{cs}}$ | $S^{\text{bg}}$ | B |
|---|---|---|---|---|---|
| $-0.15$ | $-6.92872$ | Black | $8.70060 \times 10^7$ | $4.13605 \times 10^7$ | $4.56455 \times 10^7$ |
| $-0.10$ | $-6.89194$ | Red | $1.00592 \times 10^7$ | $7.78648 \times 10^6$ | $2.27277 \times 10^6$ |
| $-0.05$ | $-6.85532$ | Green | $1.17726 \times 10^6$ | $9.75934 \times 10^5$ | $2.01329 \times 10^5$ |
| $0.00$ | $-6.81885$ | Blue | $2.18938 \times 10^2$ | $0$ | $2.18938 \times 10^2$ |
| $0.10$ | $-6.74631$ | Sky blue | $-2.61086 \times 10^4$ | $-2.63187 \times 10^4$ | $2.10070 \times 10^2$ |
| $0.15$ | $-6.71021$ | Pink | $-1.73397 \times 10^4$ | $-1.75457 \times 10^4$ | $2.05942 \times 10^2$ |
| $0.20$ | $-6.67421$ | Yellow | $-1.29572 \times 10^4$ | $-1.31591 \times 10^4$ | $2.01936 \times 10^2$ |

Table 2: The dimensionless variables and color of plot used and the actions obtained in Fig. 5.

irrespective of the value of the cosmological constant. Figure 5(a) illustrates the solution of $\tilde{\Phi}$. The upper right box in the same figure shows the magnification of the small region representing behavior of the curves which move to the left with an increase in $\tilde{U}_o$. Figure 5(b) shows $\tilde{\Phi}'$ with respect to $\tilde{\eta}$. The upper right box in the same figure shows the magnification of the small region representing behavior of the curves moving below with increasing value of $\tilde{U}_o$. Figure 5(c) illustrates the solutions of $\tilde{\rho}$. The curves move downwards with increasing value of $\tilde{U}_o$. The shape of the numerical solutions of $\tilde{\rho}$ can be easily understood if one consider a fixed space. In the fixed flat space, $\rho = \eta$. In the dS space, $\rho = \sqrt{\frac{3}{\Lambda}} \sin \sqrt{\frac{\Lambda}{3}} \eta$. In the AdS space, $\rho = \sqrt{\frac{3}{\Lambda}} \sinh \sqrt{\frac{\Lambda}{3}} \eta$. Figure 5(d) depicts the variation of $\tilde{\rho}$ with respect to $\tilde{\eta}$. The curves move below with increase in $\tilde{U}_o$. The horizontal line with $\tilde{U}_o = 0$ indicate a flat space with $\tilde{\rho}' = 1$. Table 2 shows the dimensionless variables and color of the plot used among with the action obtained from Fig. 5. From the numerical data, one can infer that the magnitude of $\tilde{\Phi}_o$ decreases as $\tilde{U}_o$ increases. We carry out the action integral in the range $0 \leqq \tilde{\eta} \leqq 30.58$ numerically. In the dS space, the solution and the background have their own periods for $\tilde{\eta}$, which we take the period as the integration limit. For the background dS space, we take $\tilde{\eta} = \pi \sqrt{\frac{3}{\tilde{\kappa}\tilde{U}_o}}$. The action for $\tilde{S}^{\text{cs}}$ and $\tilde{S}^{\text{bg}}$ are positive or zero as long as $\tilde{U}_o \leqq 0$. The background action is zero for $\tilde{U}_o = 0$. In this work, we do not check for the special case $\tilde{S}^{\text{cs}} = 0$. Simply, the action has a negative value for the dS space. It is related to the fact that the Euclidean action for Einstein gravity is not bounded from below, and this is known as the conformal factor problem in Euclidean quantum gravity [49]. It was argued in [50] that the conformal divergence due to the unboundedness of the action might get cancelled with a similar term of opposite sign caused by the measure of the path integral. However, the difference between the action of the solution and that of the background remains positive-valued.
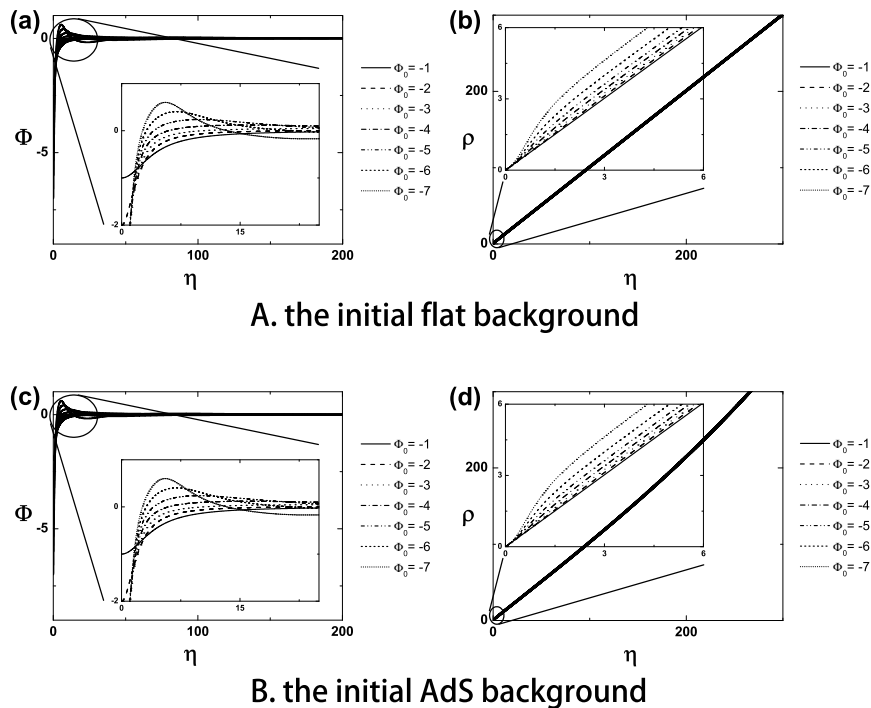
13

Figure 6: The numerical solutions representing oscillatory solutions.

## 3.2 Oscillating Fubini instantons

The oscillating instanton and the bounce solutions with an $O(4)$ symmetry between the dS-dS vacuum states was first studied in Ref. [51], in which the authors found the solutions in a fixed background geometry and showed how does the maximum allowed number $n_{\max}$ depend on the parameters of the theory, where $n$ denotes the crossing number of the potential barrier by the oscillating solutions. The oscillating bounce solutions in the presence of gravity was also studied in Ref. [52], in which the authors analyzed the negative modes and the fluctuations around the oscillating solutions. The instanton was interpreted as the thermal tunneling [53]. The oscillating instanton solutions under a symmetric double-well potential in the curved space with an arbitrary vacuum energy was also investigated in detail in [30], where a numerical solution is possible as long as the local maximum value of the potential remains positive. The solutions have a thick wall and can be interpreted as a mechanism for the nucleation of the thick wall for topological inflation [54]. Similarly, the process for the tunneling without a barrier in curved space, was studied in Ref. [28, 29]. The existence of numerical solutions was shown in Ref. [30], in which the case representing the tunneling from flat to AdS space shows an oscillating behavior. The solution oscillates around $\Phi = 0$ in the inverted potential and the

14

| $\tilde{\Phi}_0$ | $S^{\mathrm{cs}}$ (AdS) | $S^{\mathrm{bg}}$ (AdS) | B (AdS) | B (flat) |
|---|---|---|---|---|
| $-1$ | $9.03462 \times 10^5$ | $9.01815 \times 10^5$ | $1.64726 \times 10^3$ | $1.08561 \times 10^2$ |
| $-2$ | $9.05239 \times 10^5$ | $9.01815 \times 10^5$ | $3.42429 \times 10^3$ | $1.58782 \times 10^2$ |
| $-3$ | $9.07584 \times 10^5$ | $9.01815 \times 10^5$ | $5.76952 \times 10^3$ | $2.77028 \times 10^2$ |
| $-4$ | $9.10850 \times 10^5$ | $9.01815 \times 10^5$ | $9.03545 \times 10^3$ | $3.62471 \times 10^2$ |
| $-5$ | $9.16368 \times 10^5$ | $9.01815 \times 10^5$ | $1.45537 \times 10^4$ | $7.67645 \times 10^2$ |
| $-6$ | $9.26167 \times 10^5$ | $9.01815 \times 10^5$ | $2.43521 \times 10^4$ | $1.37407 \times 10^3$ |
| $-7$ | $9.47248 \times 10^5$ | $9.01815 \times 10^5$ | $4.54330 \times 10^4$ | $3.70685 \times 10^3$ |

Table 3: The dimensionless variables and color of plot used and the actions obtained in Fig. 6.

oscillating behavior die away unlike the case under a harmonic potential.

In the present paper, the oscillation means that the field in the solutions oscillates around the minimum of the inverted potential and die away asymptotically to the minimum $\Phi = 0$ for the case with $m^2 = 0$. Thus the resulting geometry of the initial state has wrinkles due to the variation of the volume energy density and the instanton simultaneously. The behavior of the solutions representing the resulting geometry with wrinkles is quite different from those in Ref. [30].

Figure 6 shows the numerical solutions representing an oscillatory behavior in (A) the initial flat background and (B) the initial AdS background. We take $\tilde{\kappa} = 0.30$, $\tilde{U}_o = 0$ (for the flat case), and $\tilde{U}_o = -0.0001$ (for the AdS case), respectively. Figures 6(a) and (c) illustrate the numerical solutions of $\tilde{\Phi}$. The lower right box in those figure shows the magnification of a small region representing the behavior of the solution around $\tilde{\Phi} = 0$. The peak corresponds to the first turning point of the particle similar to a classical mechanics problem in the presence of an inverted potential. For the case with $\tilde{\Phi}_o = -7$ the first turning point reaches furthermost point away from $\tilde{\Phi} = 0$ among all the other cases, as one can easily see from the figure. The curves oscillate around $\tilde{\Phi} = 0$ and eventually stop at $\tilde{\Phi} = 0$ in the flat and AdS space. We take the initial point as an arbitrary $\tilde{\Phi}_o$, which means that the number of oscillations for each solution can be different. However, there is the tendency that the number of oscillations is decreased as the value of $\tilde{\Phi}_o$ is decreased in the given $\tilde{\kappa}$. Figures 6(b) and (d) illustrate the numerical solutions for $\tilde{\rho}$. The upper left box in those figure shows the magnification of an initial small region representing behavior of the curves which move below with the decrease in $\tilde{\Phi}_o$.

Table 3 shows the initial values of $\tilde{\Phi}$, the actions for the AdS, and flat background which are obtained from Fig. 6. In the flat case, the background action is zero as $\tilde{U}_o = 0$ and therefore $\tilde{S}^{\mathrm{cs}}$ is equal to $\tilde{B}$. In the present case, we cut all the data at a certain point which is $\tilde{\eta} = 200$.

We now analyze the behavior of the solutions using a phase diagram method. After plugging

the value of $\frac{\rho'}{\rho}$ from Eq. (10) into Eq. (9) and using $\Phi'' = \Phi'\frac{d\Phi'}{d\Phi}$, the equation becomes

$$\frac{d\Phi'}{d\Phi} = -\frac{3\sqrt{\frac{1}{\rho^2} + \frac{\kappa}{3}(\frac{1}{2}\Phi'^2 + \frac{\lambda}{4}\Phi^4 - U_o)}\Phi' + \lambda\Phi^3}{\Phi'} \, . \tag{15}$$

First, we consider the situation where the kinetic energy is small compared to the potential energy such that $|U| \gg \Phi'^2$, $U_o \ll 1$ and the term $1/\rho^2$ is smaller than other terms. In other words, the last term is the most dominant among other terms in the numerator. Then the equation reduces to the form

$$\Phi' \simeq \sqrt{\frac{\lambda}{2}(\Phi_o^4 - \Phi^4)} \, . \tag{16}$$

The above relation shows that the first stage of the curve has got such kind of form. Second, we consider the situation where $d\Phi'/d\Phi = 0$, i.e. with vanishing acceleration and then we impose all the above mentioned conditions. It will then describe the special points in the phase diagram. Then the equation reduces to the form

$$\Phi' \simeq -2\sqrt{\frac{\lambda}{3\kappa}}\Phi \, . \tag{17}$$

Third, we consider the situation where $d\Phi'/d\Phi = -c$, i.e. a negative constant. We impose all the above mentioned conditions among with $\Phi^2 \gg 2c/\sqrt{3\kappa\lambda}$. Thus, we obtain the above equation again. This relation implies that the special points with a vanishing acceleration and some of the region with a negative constant acceleration in the phase diagram have got a linear function type behavior in the phase diagram as shown in Figs. 7(a) and (c).

Figure 7 illustrates the behavior of the solutions in the $\tilde{\Phi}$-$\tilde{\Phi}'$ plane. Each trajectory represents the behavior of the solution in the phase diagram. The trajectories begin with zero velocity as $\tilde{\Phi}' = 0$ shown in Figs. 7(a) and (c). The velocity increases rapidly to the maximum and then decreases linearly up to the turning point. Figures 7(b) and (d) show the magnification of the small region representing the behavior of the solution around $\tilde{\Phi}' = 0$ and $\tilde{\Phi} = 0$.

Basically, the Fubini solution has an asymptotic condition to be satisfied. We expect that there exist an oscillating solutions although the dS background has got a finite size in the Euclidean signature. However, if we consider an analytic continuation not of the angle parameter $\chi$ but of the Euclidean evolution parameter $\eta = it$, then the meaning becomes clearer. When there is an 'even' symmetry for the oscillating instantons, we can see the half-way point $\eta_0$ as $\dot{\rho}(\eta_0) = \dot{\Phi}(\eta_0) = 0$. Then, we can paste the Lorentzian manifold $t = 0$ at the $\eta = \eta_0$ surface. This is possible only for the case $\dot{\rho}(\eta_0) = \dot{\Phi}(\eta_0) = 0$, because of the Cauchy-Riemann theorem of complex analysis; otherwise, the Lorentzian manifold should be complex valued functions (for exceptional cases, we might be able to consider complex valued instantons, the so-called fuzzy instantons [55, 56]). In this procedure, an event shows a spontaneous creation of the universe from 'nothing' [2], in which nothing means a state without the concept of classical spacetime [57]. We already know that there is such a solution when the scalar field is exactly on top of the local maximum. However, now we observe a creation from nothing with

**A. the initial flat background**
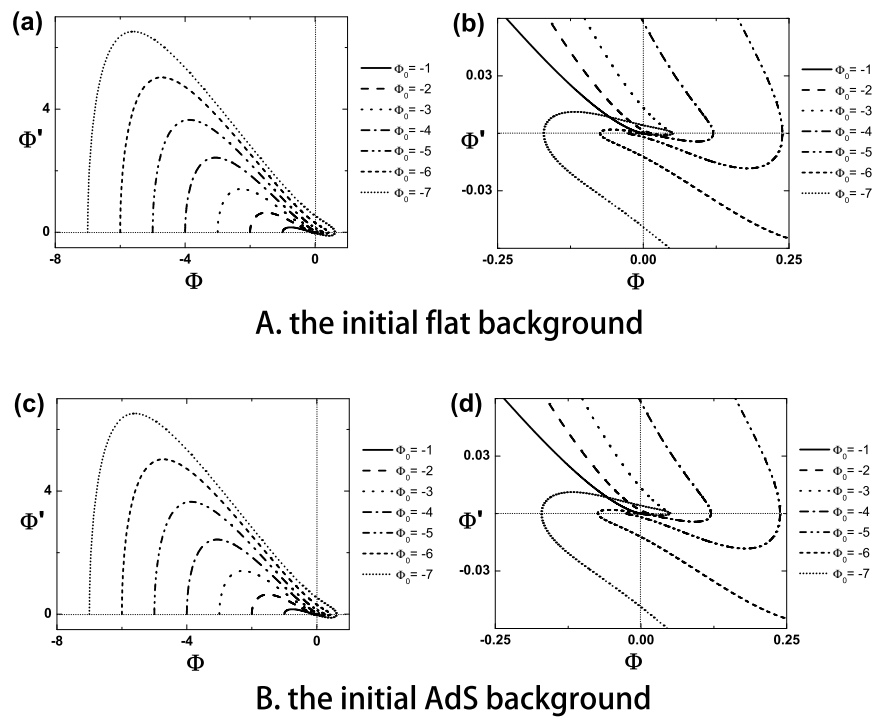
**B. the initial AdS background**

Figure 7: The behavior of the solutions represented in the phase diagram.

highly non-trivial field dynamics. This is worthwhile to be highlighted and we postpone further analysis for the future work.

## 3.3 Fubini instantons with $Z_2$ symmetry

We now shift our attention to the new type of solutions in the initial background as the dS space, i.e. $U_o > 0$. The Euclidean dS space has a compact geometry. Thus the solutions can have $Z_2$ symmetry. We consider the boundary conditions in Eq. (12). To obtain the solutions with $Z_2$ symmetry, we need to impose additional conditions. For the background geometry, $\rho' = 0$ at $\eta = \frac{\eta_{max}}{2}$. On the other hand, for the scalar field, we impose $\Phi = 0$ at $\eta = \frac{\eta_{max}}{2}$ for the solutions with odd number of crossings of the potential well and $\Phi' = 0$ at $\eta = \frac{\eta_{max}}{2}$ for the solutions with even number of crossings. The solutions with odd number of crossing have the opposite state of the value $\Phi$ at $\eta = 0$ and $\eta = \eta_{max}$, i.e. $\Phi|_{\eta=\eta_{max}} = -\Phi_o$. The solutions with even number of crossing have the same state of the value $\Phi$ at $\eta = 0$ and $\eta = \eta_{max}$, i.e. $\Phi|_{\eta=\eta_{max}} = \Phi_o$. We stress that the boundary conditions in Eq. (12) gives rise to completely new type of solutions of Fubini instanton.

Figure 8 shows the numerical solutions of the Fubini instanton with $Z_2$ symmetry. We take $\tilde{\kappa} = 0.50$ and $\tilde{U}_o = 0.03$. Thus the dS region in the $\tilde{\Phi}$-space spans the region $-0.589 \lesssim \tilde{\Phi} \lesssim 0.589$. We consider four cases with different initial positions of $\tilde{\Phi}$. Figure 8(a) illustrates the numerical solution of $\tilde{\Phi}$. The trajectories with the blue and red color go back to the same position of $\tilde{\Phi}$ in the presence of the inverted potential, i.e. they have even number of crossings. The trajectories with the black and green color go back to the opposite position of $\tilde{\Phi}$, i.e. they have odd number of crossings. Figure 8(b) depicts the numerical solution of $\tilde{\rho}$. Figures 8(c) and (d) illustrate the behavior of the solutions in the $\tilde{\Phi}$-$\tilde{\Phi}'$ plane. Each trajectory represents the behavior of the solution in the phase diagrams. The blue and red lines indicate that the interior part of two instantons has got the same state as $\tilde{\Phi}$, whereas the green and black lines indicate that the interior part has got the opposite state of $\tilde{\Phi}$. Figure 8(d) illustrates the magnification of a small region representing the behavior of the solution around $\tilde{\Phi}' = 0$ and $\tilde{\Phi} = 0$. Figure 8(e) illustrates the volume energy density, where the density has got a form $\tilde{\xi} = -\tilde{U}$. The box shows the magnification of a small region representing behavior of curves. The densities in each of the case have got positive values near the initial starting point $\tilde{\Phi}_o$ far away from the point $\tilde{\Phi} = 0$, because the densities have the form $\tilde{\xi} = -\tilde{U}$ and $\tilde{U}_o > 0$. The solutions oscillate in the dS region as found the present work. The density always negative values for the case of the black line. Figure 8(f) illustrates the Euclidean energy $\tilde{E}_{\tilde{\xi}} = 2\pi^2 \tilde{\rho}^3 \tilde{\xi}$ for each slice of constant $\tilde{\eta}$ values. The negative energy parts in each of the case signifies a rolling state in the dS region. Table 4 shows the initial value of $\tilde{\Phi}$, colors of the plot used, and the actions obtained from Fig. 8.
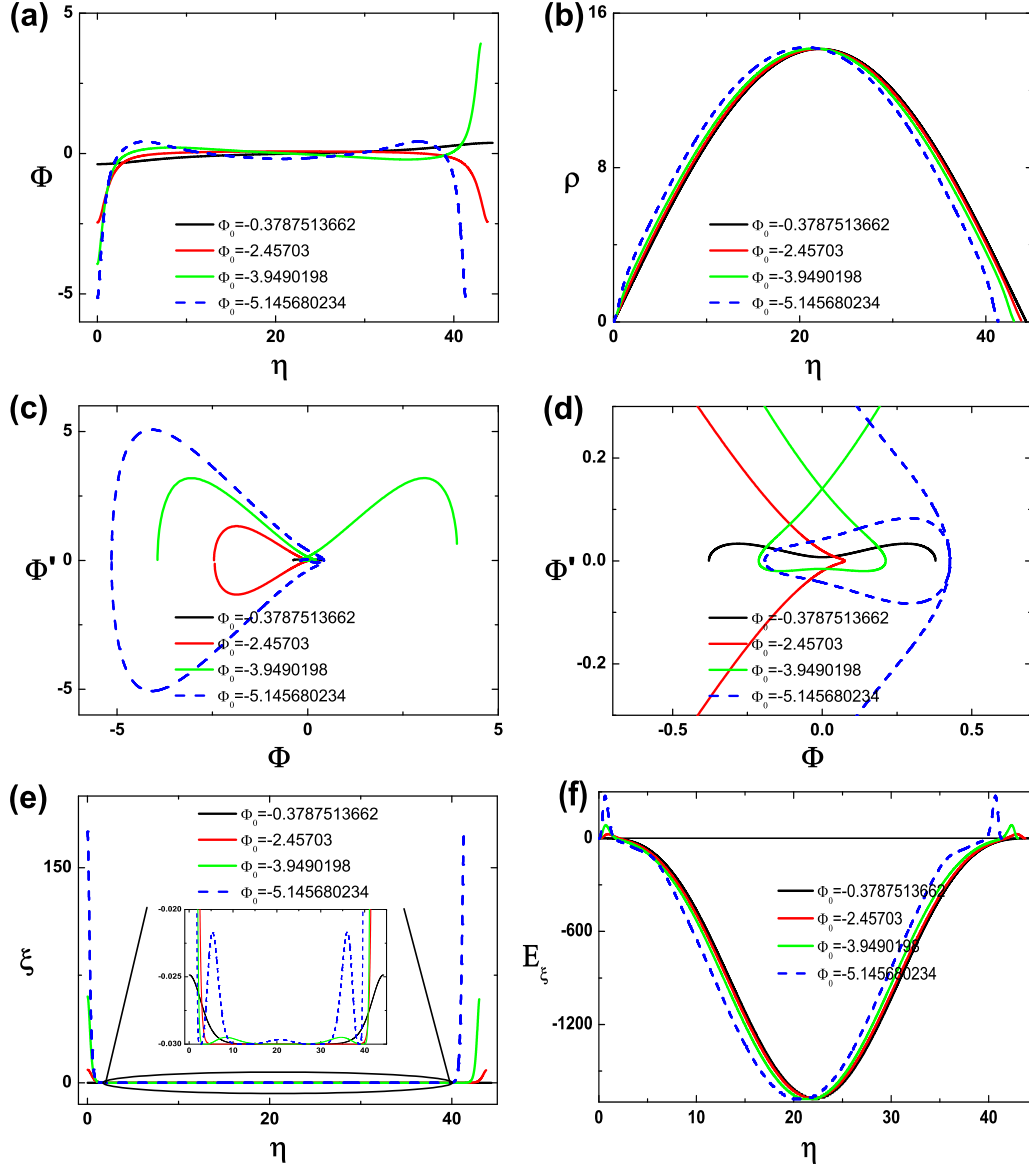
Figure 8: (color online). The numerical solutions of the Fubini instanton with $Z_2$ symmetry.

| $\tilde{\Phi}_0$ | Color of plot | $S^{\text{cs}}$ | $S^{\text{bg}}$ | B |
|---|---|---|---|---|
| $-0.37875$ | Black | $-3.15525 \times 10^4$ | $-3.15827 \times 10^4$ | 30.2 |
| $-2.45703$ | Red | $-3.15176 \times 10^4$ | $-3.15827 \times 10^4$ | 65.2 |
| $-3.94902$ | Green | $-3.14005 \times 10^4$ | $-3.15827 \times 10^4$ | 182.2 |
| $-5.14568$ | Blue | $-3.10727 \times 10^4$ | $-3.15827 \times 10^4$ | 510.0 |

Table 4: The dimensionless variables and the color of plot used, and the actions obtained in Fig. 8.

# 4   Causal structures

In this section, we briefly outline the causal structure of the solutions in the Lorentzian signature. Due to the pressure difference, the nucleated AdS region will expand over the background and hence the boundary of the nucleated AdS region will be time-like.

Figure 9 shows the schematic diagrams representing the causal structures of the Fubini instantons and the related solutions. The $\chi = \pi/2$ surface can be analytically continued to the surface $t = 0$ in the Lorentzian signature. The lower vacuum region in the instanton (green colored region) will be unstable during the Lorentzian time evolution (orange colored region). Due to the instability of the Fubini type potential, the whole causal structure may depend on the shape of the potential or the vacuum structure i.e. whether the left or the right side of the potential has true vacua or not. Therefore, the followings are meaningful only as reasonable estimations for general behavior and these may be different for special examples.

Figure 9(a) illustrates the instanton solution in an AdS background. It will form time-like $r = 0$ and $r = \infty$ boundaries in the Lorentzian signature. However, the AdS region may be unstable to form a kind of singularity. Figure 9(b) illustrates the instanton solution in the dS background. The dS region has a cosmological horizon and will this form a future infinity. The AdS region (orange colored region) will expand over the dS region due to the pressure difference. Figure 9(c) is the pair creation by the oscillating instanton solutions. Therefore, in the instanton part, the dS region around the $\rho = \rho_{\max}$ is surrounded by the AdS (green colored region) part. In the Lorentzian signature, we can interpret these two AdS parts as being nucleated in a dS background. In Fig. 9(c), we infer that, there still remains a dS region and a future infinity.

The pair creation of the instantons in this work is quite different from the ordinary quantum process of pair creation of particles. We take the initial background as the dS space, i.e. $U_o > 0$. The Euclidean dS space has a compact geometry. Thus, the geometry has two poles. If one object is created on the north pole and the other on the south pole, we can interpret that process as the pair creation of objects. As an example of the process, the two-crossing solution between the sides of the potential barrier in the double-well potential was considered as a type of a double-bounce solution or an anti-double-bounce solution [58], in which the authors
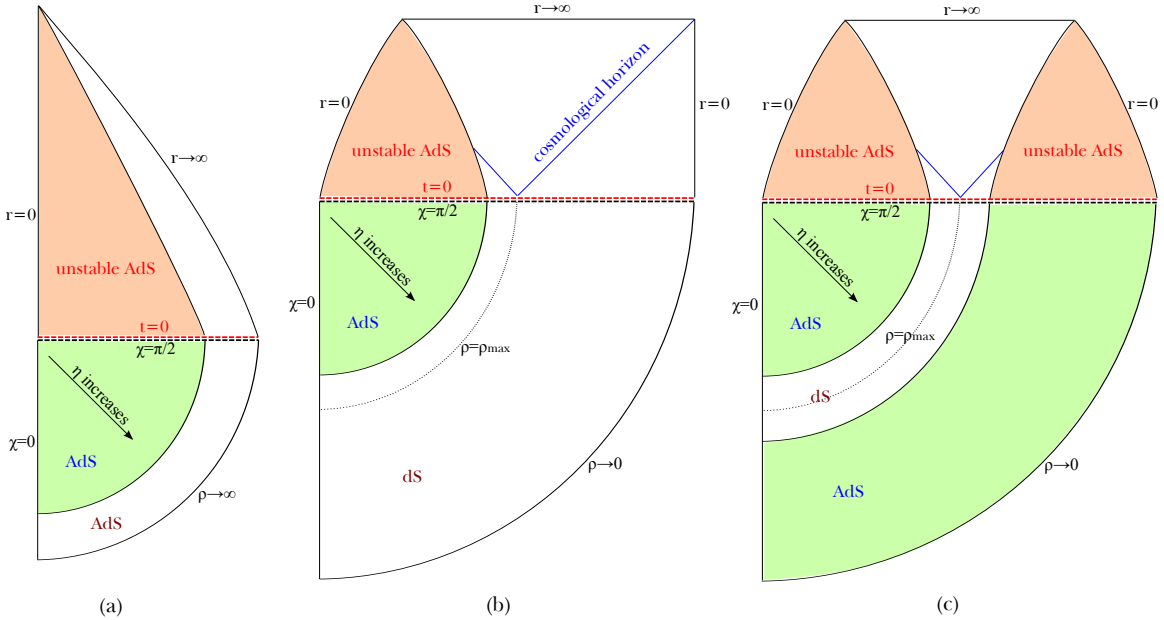
Figure 9: (color online). The schematic diagrams representing the causal structure of the Fubini instantons and the related solutions. (a) Tunneling in an AdS background. (b) oscillating instanton solution in a dS background. (c) Pair creation by oscillating instantons in dS background.

interpreted the double-bounce solution as the spontaneous pair-creation of true vacuum bubbles, one at each pole in the dS space. We adopt a similar interpretation for our solutions with $Z_2$ symmetry.

# 5   Summary and Discussions

In this paper we have studied Fubini instantons of a self-gravitating scalar field representing the tunneling without a barrier. There are two kinds of Euclidean solutions representing the tunneling without any barrier. One of them is the tunneling from the local maximum of the potential to the vacuum state. The other one is the tunneling from the maximum to any arbitrary state. The latter corresponds to the Fubini instanton solution. We have shown that there exist several new kinds of Fubini instanton solutions of a self-gravitating scalar field found as numerical solutions, which are possible only if gravity is taken into account. We also computed the action difference $B$, in each case, between the Euclidean action corresponding to a classical solution $S^{\mathrm{cs}}$ and the background action $S^{\mathrm{bg}}$ for the rate of decay.

In Sec. 2, we reviewed the Fubini instanton in the absence of gravity from the viewpoint of a tunneling problem. We have presented a numerical solution including the Euclidean energy density for example. We analyzed the structure of the solution in a theory with the potential having only a quartic self-interaction term. These solutions can be considered as a ball consisting

of only a thick wall except for the one point at the center of the solution with a lower arbitrary state than the outer vacuum state unlike a vacuum bubble which consists of an inner part with a lower vacuum state and a wall.

In Sec. 3, we have studied the instanton solutions in curved space. We performed careful numerical study to solve the coupled equations for the gravity and the scalar field simultaneously. We have shown that there exist numerical solutions without any oscillation in the initial AdS space for the potential with only the quartic term. We have also shown that there exist numerical solutions for the potential with both a quartic and a quadratic term irrespective of the value of the cosmological constant. For this particular case, there is no solution with an $O(4)$ symmetry when gravity is switched off. In order to estimate the decay rate of the background state, we calculated the action difference between the action of the solution and that of the background obtained using numerical means.

We have obtained oscillating Fubini instantons as new types of solutions. We have shown that there exist oscillating numerical solutions for the potential with only the quartic term in the flat and AdS space, except for the solution without oscillation in the initial AdS space with the specific value of a cosmological constant and the parameters. We have analyzed the behavior of the solutions using the phase diagram method. The oscillation dies away asymptotically in both the flat and the AdS space.

We have obtained numerical solutions representing the Fubini instanton with $Z_2$ symmetry. We stress that they represent completely new type of solutions of Fubini instanton. These solutions can be interpreted as the pair creation with each one having the same state and with each one having the opposite state, respectively. The solutions can lead to more interesting interpretation as follows: any arbitrary state can tunnel into another arbitrary state with an $O(4)$-symmetry in the curved spacetime, although no vacuum state exists as the instanton solution. The solutions are possible as long as the maximum of the potential remains positive.

The subject on the pair creation of bubbles was first considered in Ref. [59]. The numerical solution representing the pair of solutions is in Fig. 2 in Ref. [58], which can be interpreted as the pair creation of the bubbles, one at each pole in the dS space. However, there is a different interpretation on the solutions [53, 60], in which the authors studied a decay channel of de Sitter vacua. The solutions with $O(3)$ symmetry can be understood as describing tunneling in a finite horizon volume at finite temperature. The solutions maybe correspond to thermal production of a bubble in their interpretation. In this stage, the comparative analysis between the O(4)-symmetric solution and O(3)-symmetric solution with respect to the pair creation is needed to be studied more. We leave this for future work.

In Sec. 4, we have analyzed the schematic diagrams representing the causal structures of the Fubini instantons and the related solutions in the Lorentzian signature. For the special case representing the solution with $Z_2$ symmetry, the dS region around the $\rho = \rho_{\max}$ is surrounded by an AdS part.

We now mention on the negative mode problem. It was known that the bounce solution has one negative mode in the spectrum of small perturbations about the solution [46, 61]. The

bounce solution with one negative mode corresponds to the tunneling process in the lowest WKB approximation. In Ref. [61], Coleman argued that the Euclidean solution with only one negative mode is related to the tunneling process in the flat Minkowski spacetime. However, there is no rigorous proof on extension of Coleman's argument to the curved space claiming the physical irrelevance of the solutions with additional negative modes. For example, the time-translation invariance, or zero modes, is one of crucial elements to prove the uniqueness of the negative mode in his argument. However, the existence of zero modes is not guaranteed in curved spacetime. Another point is that the Euclidean time interval is at most of $O(H^{-1})$ in de Sitter space. Hence, only a finite number of the bounces can be placed far apart from each other. Therefore, the dilute gas approximation may become invalid easily, which leads to the breakdown of the WKB approximation [62]. There appears diverse situations on the negative modes when the gravity is taken into account [62–65]. Although, the bounce solution with one negative mode in curved space dominates the tunneling process, the solutions with additional negative modes may also contribute to the tunneling process. There exist some works including the physical interpretation on the oscillating solutions with more than one negative mode. One can naturally interpret the system in de Sitter background as a thermal system. The authors in Refs. [51,53] interpreted that the existence of additional negative modes represents the solutions as unstable intermediate thermal configuration. They seem to observe the clue to support this idea on the other point of view. It is known that the $N$ times oscillating solutions have $N$ negative modes [51,53,66]. The even numbers of negative modes of the form $4N$ and $4N+2$ do not have imaginary part of the energy, while the odd numbers of negative modes of the form $4N+3$ have the imaginary part of the energy with the wrong sign. However, $4N+1$ negative modes may have a meaning for a tunneling process even if the solution may not be related to the lowest WKB approximation. Recently the analysis on the negative modes of oscillating instantons has been investigated [66]. The oscillating instantons as homogeneous tunneling channels have been also studied [67]. In conclusion, we believe many Euclidean solutions in curved space with zero and negative modes may have physical significance and deserves further investigation.

In summary, we illustrate the following finding in our new contribution regarding this issue:

1. In the absence of gravity, a $-\phi^4$-type potential has infinitely many instanton solutions whereas a $-\phi^4 + \phi^2$-type potential has no instanton solution. However, *the inclusion of the gravity changes all the situation abruptly*: for the former case, the solution space get reduced to a finite space and for the latter case, there exists solutions.

2. We also confirm that $-\phi^4$-type potentials have oscillating instanton solutions as well as the solutions with $Z_2$ symmetry.

Therefore, the Fubini instanton is one of the few examples that shows the effect of gravity bringing drastic changes to the tunneling process. There can be more applications of the oscillating instantons and we confirm that the Fubini-type potentials also contribute largely towards these processes. We postpone any possible application of such oscillating solutions including the phase space of solutions for our future work [48].

# 6   Acknowledgements

# References

[1] A. D. Linde, *Nonsingular regenerating inflationary universe*, Cambridge University preprint, Print-82-0554.

[2] A. Vilenkin, Phys. Rev. D **27**, 2848 (1983); arXiv: gr-qc/0409055.

[3] A. D. Linde, Phys. Lett. B **175**, 395 (1986).

[4] A. H. Guth, Phys. Rep. **333-334**, 555 (2000).

[5] S. Winitzki, Lect. Notes Phys. **738**, 157 (2008).

[6] R. Bousso and J. Polchinski, J. High Energy Phys. 06 (2000) 006.

[7] L. Susskind, arXiv: hep-th/0302219.

[8] J. Garriga and A. Vilenkin, Phys. Rev. D **57**, 2230 (1998).

[9] A. Borde, A. H. Guth, and A. Vilenkin, Phys. Rev. Lett. **90**, 151301 (2003).

[10] A. Mithani and A. Vilenkin, arXiv:1204.4658; L. Susskind, arXiv:1204.5385; arXiv:1205.0589.

[11] S. Kachru, R. Kallosh, A. Linde, and S. P. Trivedi, Phys. Rev. D **68**, 046005 (2003).

[12] S. K. Ashok and M. R. Douglas, J. High Energy Phys. 01 (2004) 060.

[13] C. M. Hull, Classical Quantum Gravity **2**, 343 (1985).

[14] R. Kallosh, A. Linde, S. Prokushkin, and M. Shmakova, Phys. Rev. D **65**, 105016 (2002); *ibid.* D **66**, 123503 (2002).

[15] R. Kallosh and A. Linde, Phys. Rev. D **67**, 023510 (2003).

[16] H. Kim, J. High Energy Phys. 01 (2003) 080.

[17] A. A. Belavin, A. M. Polyakov, A. S. Schwartz, and Yu. S. Tyupkin, Phys. Lett. **59B**, 85 (1975).

[18] S. Coleman, *Aspects of symmetry* (Cambridge University Press, Cambridge, England, 1985).

[19] I. Herbut, *A Modern Approach to Critical Phenomena* (Cambridge University Press, Cambridge, 2007).

[20] M. B. Voloshin, I. Yu. Kobzarev, and L. B. Okun, Yad. Fiz. **20**, 1229 (1974) [Sov. J. Nucl. Phys. **20**, 644 (1975)].

[21] S. Coleman, Phys. Rev. D **15**, 2929 (1977); *ibid.* D **16**, 1248(E) (1977).

[22] S. Coleman and F. De Luccia, Phys. Rev. D **21**, 3305 (1980).

[23] S. Parke, Phys. Lett. **121B**, 313 (1983).

[24] K. Lee and E. J. Weinberg, Phys. Rev. D **36**, 1088 (1987).

[25] B.-H. Lee and W. Lee, Classical Quantum Gravity **26**, 225002 (2009).

[26] S. Fubini, Nuovo Cimento A **34**, 521 (1976).

[27] A. D. Linde, Nucl. Phys. **B216**, 421 (1983); *ibid.* **B223**, 544(E) (1983).

[28] K. Lee and E. J. Weinberg, Nucl. Phys. **B267**, 181 (1986); K. Lee, Nucl. Phys. **B282**, 509 (1987).

[29] L. G. Jensen and P. H. Steinhardt, Nucl. Phys. **B317**, 693 (1989).

[30] B.-H. Lee, C. H. Lee, W. Lee, and C. Oh, Phys. Rev. D **85**, 024022 (2012).

[31] S. Kanno, M. Sasaki, and J. Soda, Classical Quantum Gravity **29**, 075010 (2012); Prog. Theor. Phys. **128**, 213 (2012).

[32] J. Garriga, X. Montes, M. Sasaki, and T. Tanaka, Nucl. Phys. B **551**, 317 (1999).

[33] S. Khlebnikov, Nucl. Phys. B **631**, 307 (2002).

[34] F. Loran, Mod. Phys. Lett. A **22**, 2217 (2007).

[35] S. de Haro and A. C. Petkou, J. High Energy Phys. 12 (2006) 076; S. de Haro, I. Papadimitriou, and A. C. Petkou, Phys. Rev. Lett. **98**, 231601 (2007).

[36] J. L. F. Barbon and E. Rabinivici, J. High Energy Phys. 04 (2010) 123; J. High Energy Phys. 04 (2011) 044.

[37] A. N. Kuznetsov and P. G. Tinyakov, Mod. Phys. Lett. A **11**, 479 (1996); Phys. Rev. D **56**, 1156 (1997).

[38] A. A. Yurova and A. V. Yurov, Phys. Lett. A **372**, 4222 (2008).

[39] C. M. Bender and T. T. Wu, Phys. Rev. D **7**, 1620 (1973); J.-Q. Liang and H. J. W. Müller-Kirsten, Phys. Rev. D **45**, 2963 (1992); *ibid.* D **48**, 964(E) (1993).

[40] L. N. Lipatov, Sov. Phys. JETP **45**, 216 (1977).

[41] I. Affleck, Nucl. Phys. **B191**, 429 (1981).

[42] J. W. York, Jr., Phys. Rev. Lett, **28**, 1082 (1972); G. W. Gibbons and S. W. Hawking, Phys. Rev. D **15**, 2752 (1977); J. W. York, Jr., Found. Phys. **16**, 249 (1986).

[43] C. W. Misner, K. S. Thorne, and J. A. Wheeler, *Gravitation* (Freeman, San Francisco, 1973).

[44] B. K. Berger, Gen. Rel. Grav. **38**, 625 (2006).

[45] W. H. Press, S. A. Teukolsky, W. T. Vetterling, and B. P. Flannery, *Numerical Recipes in Fortran* (Cambridge University Press, Cambridge, England, 1992).

[46] C. G. Callan, Jr. and S. Coleman, Phys. Rev. D **16**, 1762 (1977).

[47] E. J. Weinberg, Phys. Rev. D **47**, 4614 (1993); J. Baacke and G. Lavrelashvili, Phys. Rev. D **69**, 025009 (2004); G. V. Dunne and H. Min, Phys. Rev. D **72**, 125004 (2005).

[48] B.-H. Lee, W. Lee, D. Ro, and D.-h. Yeom, in progress.

[49] G. W. Gibbons, S. W. Hawking, and M. J. Perry, Nucl. Phys. **B138**, 141 (1978).

[50] A. Dasgupta and R. Loll, Nucl. Phys. B **606**, 357 (2001).

[51] J. C. Hackworth and E. J. Weinberg, Phys. Rev. D **71**, 044014 (2005); E. J. Weinberg, AIP Conf. Proc. **805**, 259 (2005).

[52] G .V. Lavrelashvili, Phys. Rev. D **73**, 083513 (2006); G. V. Dunne and Q.-h. Wang, Phys. Rev. D **74**, 024018 (2006).

[53] A. R. Brown and E. J. Weinberg, Phys. Rev. D **76**, 064003 (2007).

[54] A. Vilenkin, Phys. Rev. Lett. **72**, 3137 (1994); A. Linde, Phys. Lett. B **327**, 208 (1994).

[55] J. B. Hartle, S. W. Hawking, and T. Hertog, Phys. Rev. Lett. **100**, 201301 (2008); Phys. Rev. D **77**, 123537 (2008).

[56] D.-i. Hwang, H. Sahlmann, and D.-h. Yeom, Classical Quantum Gravity **29**, 095005 (2012); D.-i. Hwang, B.-H. Lee, H. Sahlmann, and D.-h. Yeom, Classical Quantum Gravity **29**, 175001 (2012).

[57] A. Vilenkin, Nucl. Phys. **B252**, 141 (1985).

[58] R. Bousso and A. Linde, Phys. Rev. D **58**, 083503 (1998).

[59] J. Garriga and A. Megevand, Phys. Rev. D **69**, 083510 (2004); Int. J. Theor. Phys. **43**, 883 (2004).

[60] A. Masoumi and E. J. Weinberg, Phys. Rev. D **86**, 104029 (2012).

[61] S. R. Coleman, Nucl. Phys. **B298**, 178 (1988).

[62] T. Tanaka and M. Sasaki, Prog. Theor. Phys. **88**, 503 (1992); T. Tanaka, Nucl. Phys. **B556**, 373 (1999).

[63] A. R. Brown and A. Dahlen, Phys. Rev. D **84**, 105004 (2011).

[64] G. V. Lavrelashvili, V. A. Rubakov, and P. G. Tinyakov, Phys. Lett. **161B**, 280 (1985).

[65] A. Khvedelidze, G. Lavrelashvili, and T. Tanaka, Phys. Rev. D **62**, 083501 (2000); G. Lavrelashvili, Nucl. Phys. B, Proc. Suppl. **88**, 75 (2000).

[66] L. Battarra, G. Lavrelashvili and J.-L. Lehners, Phys. Rev. D **86**, 124001 (2012).

[67] B.-H. Lee, W. Lee, and D.-h. Yeom, arXiv:1206.7040 [hep-th].